OPEN ACCESS
Fractals, Vol. 30, No. 10 (2022) 2240194 (11 pages)

DOI: 10.1142/S0218348X22401946

INTERLAYER AND INTRALAYER SYNCHRONIZATION IN MULTIPLEX FRACTIONAL-ORDER NEURONAL NETWORKS

BO YAN
School of Information Engineering
Shaoyang University, Shaoyang 422000, P. R. China

FATEMEH PARASTESH
Department of Biomedical Engineering
Amirkabir University of Technology (Tehran Polytechnic)
Tehran, Iran

SHAOBO HE*
School of Physics and Electronics
Central South University, Changsha 410083, P. R. China
heshaobo@csu.edu.cn

KARTHIKEYAN RAJAGOPAL
Centre for Nonlinear Systems
Chennai Institute of Technology, Chennai 600069, India

SAJAD JAFARI
Department of Biomedical Engineering
Amirkabir University of Technology (Tehran Polytechnic)
Tehran, Iran

*Corresponding author.

Health Technology Research Institute
Amirkabir University of Technology (Tehran Polytechnic)
Tehran, Iran

MATJAŽ PERC
Faculty of Natural Sciences and Mathematics
University of Maribor, Koroška cesta 160
2000 Maribor, Slovenia

Complexity Science Hub Vienna, Josefstädterstraße 39
1080 Vienna, Austria

Department of Medical Research
China Medical University Hospital
China Medical University, 404332
Taichung, Taiwan

Alma Mater Europaea, Slovenska ulica 17
2000 Maribor, Slovenia

Received December 12, 2021
Accepted March 21, 2022
Published October 19, 2022

Abstract

Fractional-order models describing neuronal dynamics often exhibit better compatibility with diverse neuronal firing patterns that can be observed experimentally. Due to the overarching significance of synchronization in neuronal dynamics, we here study synchronization in multiplex neuronal networks that are composed of fractional-order Hindmarsh–Rose neurons. We compute the average synchronization error numerically for different derivative orders in dependence on the strength of the links within and between network layers. We find that, in general, fractional-order models synchronize better than integer-order models. In particular, we show that the required interlayer and intralayer coupling strengths for interlayer or intralayer synchronization can be weaker if we reduce the derivative order of the model describing the neuronal dynamics. Furthermore, the dependence of the interlayer or intralayer synchronization on the intralayer or interlayer coupling strength vanishes with decreasing derivative order. To support these results analytically, we use the master stability function approach for the considered multiplex fractional-order neuronal networks, by means of which we obtain sufficient conditions for the interlayer and intralayer synchronizations that are in agreement with numerical results.

Keywords: Fractional-Order Neuron Model; Neuronal Network; Multiplex Network; Synchronization; Master Stability Function.

1. INTRODUCTION

Fractional-order differential equations provide a more realistic description of many actual behaviors.[1] Consequently, fractional calculus has been widely used to model diverse dynamical systems.[2–4] One advantage of the fractional-order modeling is its ability to consider the memory effect in processes.[5] Fractional differentiation has been comprehensively considered in different areas like physics and biology.[6–10] The studies have revealed that the signal propagation in neurons can be well expressed by using fractional-order derivatives.[11] Therefore, fractional neuronal models have received substantial attention.[12–14] For example,

Mondal *et al.*[15] analyzed a FitzHugh–Rinzel neuron model for different fractional derivatives and found diverse firing patterns. Jun *et al.*[16] studied the responses of the fractional Hindmarsh–Rose (HR) system. Their analysis represented that with decreasing the derivative order, the Hopf bifurcation point becomes larger, and the frequency of the firings increases.

One of the most critical problems in the study of the neurons' behaviors is their synchronous firing. Synchronization is a global phenomenon discovered in a variety of dynamic systems.[17] In the brain, synchronization plays significant roles, including information processing and cognitive tasks.[18] Hence, most of the previous researches have been devoted to the synchronous behavior of coupled neurons.[19–21] Belykh *et al.*[22] represented that stable synchronization in bursting neurons is related to their receiving signals. While the synchronization of the linearly coupled neurons only depends on the network topology. Uzuntarla *et al.*[23] studied the synchronization of the bistable neurons under different synaptic connections. They showed that the strong synchronization in the excitatory coupled neurons leads to a spontaneous termination of the neurons' activities. Recently, researchers have also considered the impact of different relating factors on the neurons' synchronization. Some of these factors are the electromagnetic field effects,[24,25] the time delay,[26] the temperature,[27] the autapse,[28] etc. Among the studies, there are also some works focusing on the synchronization of fractional-order neuron models.[29–32] Malik and Mir[33] studied the synchronous behavior of two HR systems with fractional derivatives and evaluated their robustness against the noise. Giresse *et al.*[34] investigated how the derivatives' order impact on the synchronization of the network of extended HR neurons. They realized that the fractional derivative results in fast synchronization. Meng *et al.*[35] considered time-delay fractional-order neurons with electromagnetic induction and derived sufficient conditions for their synchronization analytically.

With the advancement of complex network science, researchers have attended to networks with more complex structures.[36] A multilayer network is one of the complex structures that provides a proper representation for many natural systems.[37] The multilayer structure allows for considering multiple interactions among systems. Therefore, the synchronizability of multilayer networks has grabbed considerable attention in different fields such as neuroscience.[38–40] For instance, Xu *et al.*[41] considered the synchronous behavior of the memristive neurons in a multilayer network. Shafiei *et al.*[42] focused on synchrony between neurons in a three-layer structure with different synaptic connections. They found opposed synchronization behavior for weak and strong couplings. Rakshit *et al.*[43] explored the synchronization of neurons locating in two layers with time-varying intralayer topology. They presented the necessary conditions for the interlayer and intralayer synchronizations using linear stability analysis.

Here, the occurrence of synchronization is under consideration in coupled fractional-order neuron models with multiplex structure. The network is constructed by two layers of small-world structures with identical neurons but non-identical connections. The order of the derivatives and the coupling strengths between and within the layers are the control parameters. The intralayer and the interlayer synchronizations are analyzed by numerical simulations of the network. Then the necessary conditions for synchronizations are derived by extending the master stability function approach to the coupled fractional-order systems in the multiplex framework.

2. THE MODEL

A multiplex network of HR systems with fractional derivatives is considered. The dynamics of model is described by

$$\begin{aligned} D_t^\alpha x &= y + 3x^2 - x^3 - z + I_{\text{ext}}, \\ D_t^\alpha y &= c - 5x^2 - y, \\ D_t^\alpha z &= r(s(x + 1.6) - z), \end{aligned} \tag{1}$$

where D_t^α denotes the α order fractional derivative. The parameters of the model are set at $I_{\text{ext}} = 3.2$, $r = 0.006$, $s = 4$. The firing pattern of model relies on the derivative order α. The bifurcation of the system equation (1) according to the derivative order is demonstrated in Fig. 1a. It can be seen that with a decrement in the derivative order, the peak of the oscillations reduces. Furthermore, the frequency of the spikes in the bursts first increases until $\alpha = 0.934$ and then decreases. Some examples of the time series of the neuron for $\alpha = 1, 0.95, 0.9, 0.85, 0.8, 0.75, 0.7$ are shown in

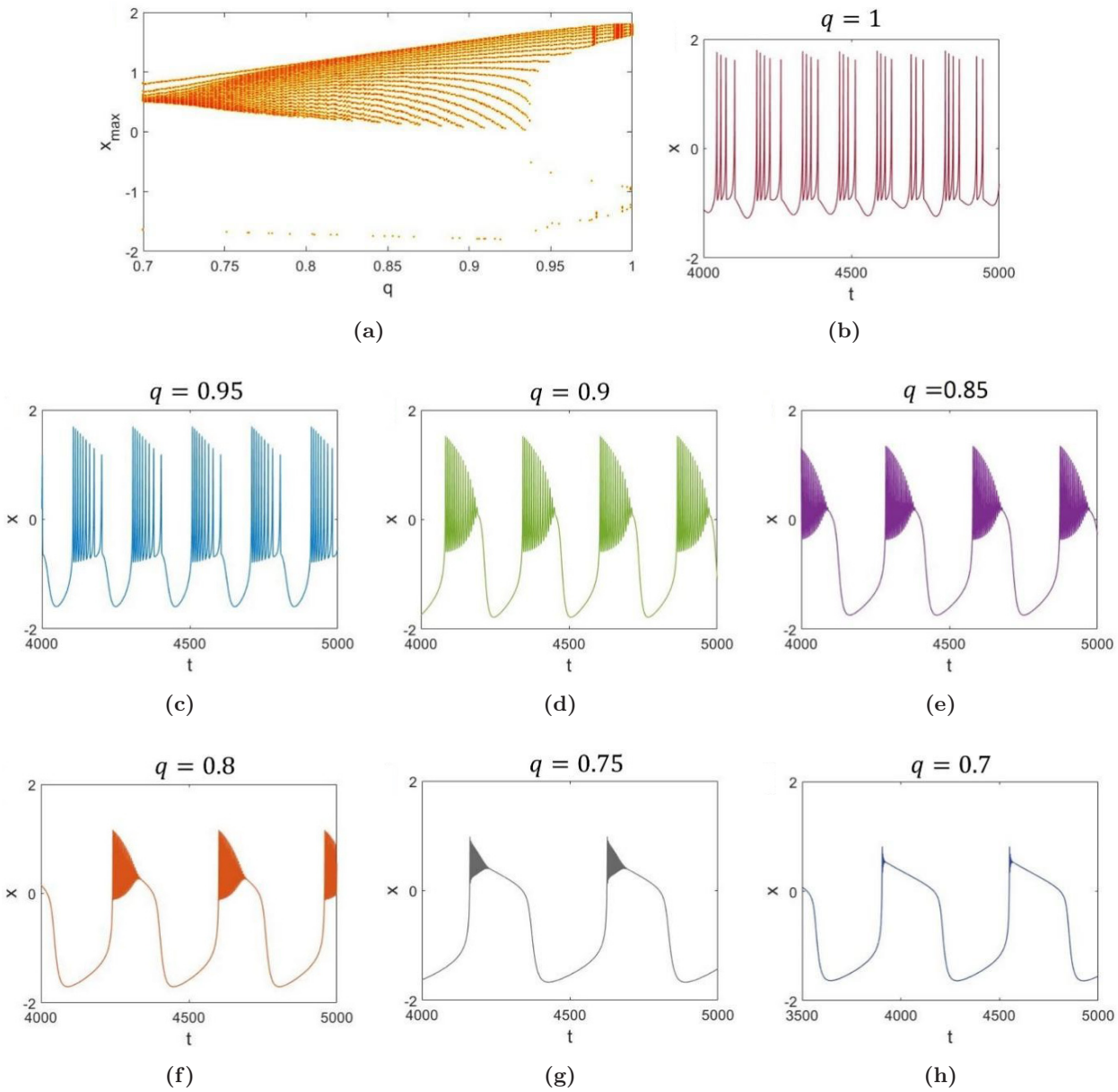

Fig. 1 **(a)** The bifurcation diagram of the fractional-order HR neuron (Eq. (1)) according to the fractional-order α, **(b)–(h)** the wave form of the system (Eq. (1)) for different fractional-order derivatives; **(b)** $\alpha = 1$, **(c)** $\alpha = 0.95$, **(d)** $\alpha = 0.9$, **(e)** $\alpha = 0.85$, **(f)** $\alpha = 0.8$, **(g)** $\alpha = 0.75$, **(h)** $\alpha = 0.7$. As α decreases, the frequency of spikes in bursts first increases and then decreases. While, the frequency of the bursts decreases.

Figs. 1b–1h. It can be seen that as α decreases, the shape of the time series changes from square-wave burster to triangular burster. Moreover, the period of the bursts increases.

$N = 100$ neurons construct each network layer with the small-world structure with probability 0.1 and 10 nearest neighbors' connections. Every node in the first layer is linked with its replica in the second layer. Figure 2 represents a delineative diagram of the network. The equations describing the network can be given as

$$\begin{aligned} D_t^\alpha X_i &= F(X_i) + \sigma \sum_{j=1}^{N} G_{ij}^1 h(X_j) \\ &\quad + \epsilon[H(Y_i) - H(X_i)], \\ D_t^\alpha Y_i &= F(Y_i) + \sigma \sum_{j=1}^{N} G_{ij}^2 h(Y_j) \\ &\quad + \epsilon[H(X_i) - H(Y_i)], \end{aligned} \tag{2}$$

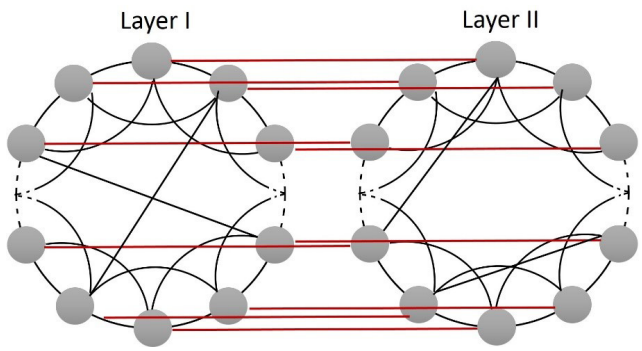

Fig. 2 The schematic of the network that consists of two layers of $N = 100$ neurons with a small-world structure. The back and the red links show the intralayer and the interlayer connections with strength σ and ϵ, respectively.

where X_i and Y_i, $i = 1, \ldots, N$ are the m-dimensional state variable of the systems in the first and second layers. D_t^α denotes the α order fractional derivative, $F(X_i)$ is the dynamics of the single HR system as Eq. (1), σ and ϵ are the intralayer and interlayer coupling strengths. The connection matrixes are denoted by $G^1 = [G^1_{ij}]_{N\times N}$ and $G^2 = [G^2_{ij}]_{N\times N}$, which are zero-row-sum matrixes with $G_{ij} = 1$ if the nodes i and j are linked, and $G_{ij} = 0$, else. The inner coupling functions are shown by $h(X)$ and $H(X)$, which are assumed to be linear through x variables, thus $h(X) = H(X) = \begin{bmatrix} x & 0 & 0 \\ 0 & 0 & 0 \\ 0 & 0 & 0 \end{bmatrix}$. The paper aims to find the effects of the strength of the connections (σ,ϵ) and the derivative order (α) on the synchrony of the neurons.

3. RESULTS

The two-layer network is solved for different derivative orders, and the emergence of synchronization within and between the layers is considered by varying the coupling strengths. The fourth-order Runge–Kutta is applied to solve integer-order equations. The fractional-order model is considered based on the Caputo fractional derivative operator. For a given fractional differential equation as

$$\begin{aligned} &{}_0^C D_t^\alpha x(t) = F(t, x(t)), \\ &x(0) = x_0, \end{aligned} \tag{3}$$

${}_0^C D_t^\alpha$ expresses the α Caputo fractional order as

$$\begin{aligned} &{}_0^C D_t^\alpha x(t) = \frac{1}{\Gamma(n-\alpha)} \int_0^t f^n(\tau)(t-\tau)^{n-\alpha-1} d\tau, \\ &n-1 < \alpha < n, \quad n \in N. \end{aligned} \tag{4}$$

For the numerical solving of the fractional-order equations the Adams–Bashforth–Moulton method described in Ref. 44 is used.

In the following sections, the appearance of intralayer and interlayer synchronizations in the network is investigated.

3.1. Intralayer Synchronization

Intralayer synchronization occurs when the neurons within the layers become synchronous. To evaluate the intralayer synchronization numerically, the averaged intralayer synchronization error is computed as follows:

$$E_X = \lim_{T\to\infty} \frac{1}{T} \int_0^T \sum_{j=2}^{N} \frac{\|X_j(t) - X_i(t)\|}{N-1} dt, \tag{5}$$

where $\|.\|$ represents the Euclidean norm, and T is a long duration of time. Figure 3 represents the intralayer synchronization error for different derivative orders. Figure 3a shows that the intralayer synchronization in the integer-order model depends on both coupling strengths (σ and ϵ). It can be seen that when ϵ increases from 0.1 to 0.4, the intralayer error decays to zero for lower σ. But when ϵ reaches 0.5, the synchrony threshold (zero error point) becomes larger. Thus, by increasing ϵ, the required intralayer coupling strength (σ) for intralayer synchronization first decreases and then increases. By changing the derivatives to the fractional order, the trend of the error changes. For $\alpha = 0.9$ (Fig. 3a), the intralayer synchronization is obtained for lower σ than the integer-order case. Furthermore, the dependence on the interlayer coupling strength decreases such that the zero points of error are almost the same for all ϵ values. Figures 3c and 3d show that the dependence of intralayer synchrony on ϵ decreases for lower orders. Moreover, for $\alpha = 0.8$, the intralayer synchrony is achieved for slightly lower σ than $\alpha = 0.9$. While for $\alpha = 0.7$, more σ is needed for synchrony.

To confirm the results of the synchronization error, the necessary conditions for the synchronization of the network are also derived by applying the master stability function method. We consider the synchronization within the layers, regardless of the synchronization between two layers. Assuming the synchronous manifold of the first layer and the second layer to be $S_X(t)$ and $S_Y(t)$, thus, $X_i(t) = S_X(t)$ and $Y_i(t) = S_Y(t)$ for $i = 1, \ldots, N$,

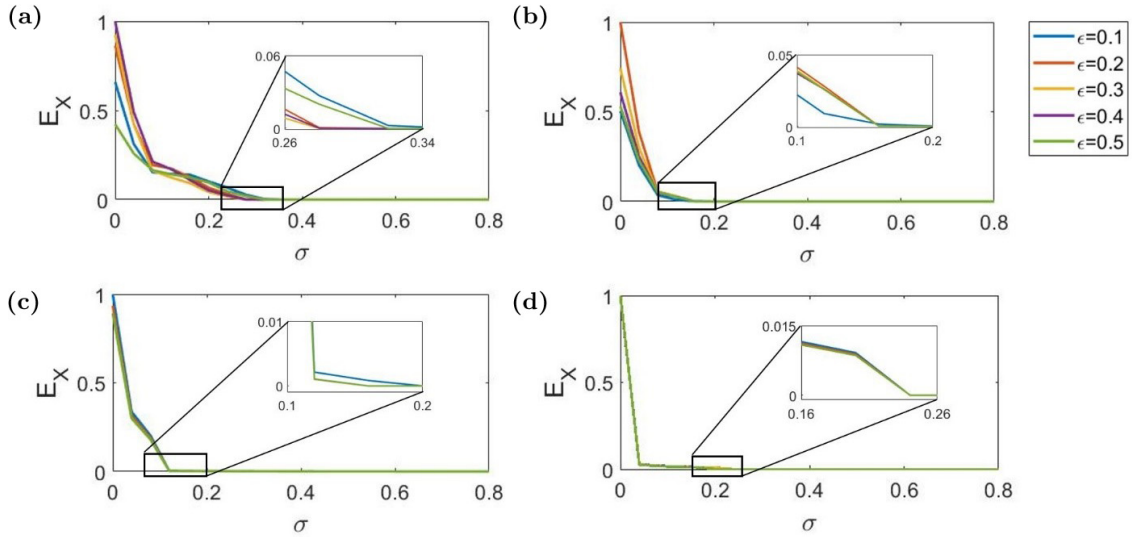

Fig. 3 The intralayer synchronization error according to intralayer coupling strength (σ), for different interlayer coupling strengths (blue: $\epsilon = 0.1$, red: $\epsilon = 0.2$, yellow: $\epsilon = 0.3$, purple: $\epsilon = 0.4$, green: $\epsilon = 0.5$). **(a)** $\alpha = 1$; **(b)** $\alpha = 0.9$; **(c)** $\alpha = 0.8$; **(d)** $\alpha = 0.7$. With decreasing α, the intralayer synchronization is achieved in weaker couplings.

where

$$\begin{aligned} D_t^\alpha S_X &= F(S_X) + \epsilon[H(S_Y) - H(S_X)], \\ D_t^\alpha S_Y &= F(S_Y) + \epsilon[H(S_X) - H(S_Y)]. \end{aligned} \tag{6}$$

Then the perturbations from the synchronous manifold can be defined as $\delta X_i = X_i - S_X$ and $\delta Y_i = Y_i - S_Y$. By derivation of the perturbed equations, we get $D_t^\alpha \delta X_i = D_t^\alpha X_i - D_t^\alpha S_X$ and $D_t^\alpha \delta Y_i = D_t^\alpha Y_i - D_t^\alpha S_Y$. Thus, the linearized equations can be obtained as follows:

$$\begin{aligned} D_t^\alpha \delta X_i &= JF(S_X)\delta X_i + \sigma \sum_{j=1}^{N} G_{ij}^1 Jh(S_X)\delta X_j \\ &\quad + \epsilon[JH(S_Y)\delta Y_i - JH(S_X)\delta X_i], \\ D_t^\alpha \delta Y_i &= JF(S_Y)\delta Y_i + \sigma \sum_{j=1}^{N} G_{ij}^2 Jh(S_Y)\delta Y_j \\ &\quad + \epsilon[JH(S_X)\delta X_i - JH(S_Y)\delta Y_i]. \end{aligned} \tag{7}$$

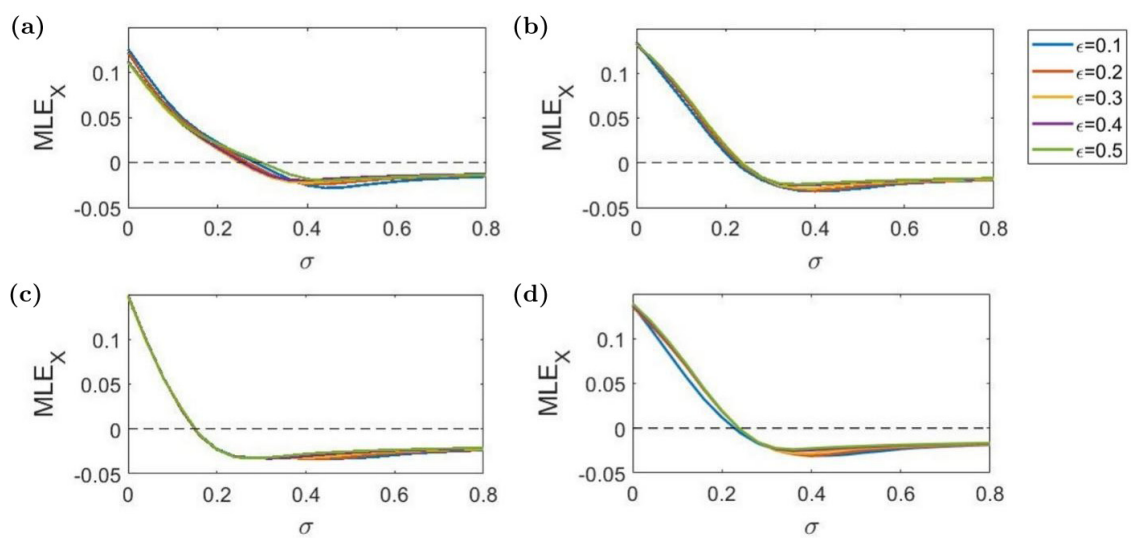

Fig. 4 The MLE of the linearized equations obtained for the intralayer synchronization (Eq. (7)) according to intralayer coupling strength (σ), for different interlayer coupling strengths (blue: $\epsilon = 0.1$, red: $\epsilon = 0.2$, yellow: $\epsilon = 0.3$, purple: $\epsilon = 0.4$, green: $\epsilon = 0.5$). **(a)** $\alpha = 1$; **(b)** $\alpha = 0.9$; **(c)** $\alpha = 0.8$; **(d)** $\alpha = 0.7$.

The maximum Lyapunov exponent (MLE) of the linearized system (Eq. (7)), which is transverse to the synchronous manifold (S_X and S_Y) specifies the stability of the intralayer synchrony. When MLE $<$ 0, the linearized perturbation system is stable about zero equilibrium point and thus, the intralayer synchronization is stable.

Figure 4 shows the MLE of Eq. (7) by altering the intralayer coupling strength (σ) for different derivative orders. It is observed that by reducing the fractional order, the required σ for intralayer synchronization decreases until $\alpha = 0.8$ and then increases for $\alpha = 0.7$. The dependence of the MLE on ϵ also reduces with decreasing α. These results are well matched with the ones obtained from the numerical intralayer synchronization error.

3.2. Interlayer Synchronization

The interlayer synchronization is known as the synchrony between the corresponding nodes in two layers, regardless of the synchrony within layers. The interlayer synchronization error is found by

$$E_{XY} = \lim_{T\to\infty} \frac{1}{T} \int_0^T \sum_{j=1}^{N} \frac{\|Y_j(t) - X_j(t)\|}{N} dt, \qquad (8)$$

with $\|.\|$ being the Euclidean norm and T as a long time interval. The interlayer synchronization error for $\alpha = 1, 0.9$ and 0.8 is demonstrated in Fig. 5. Figure 5a shows that for $\sigma = 0.05$, the interlayer synchronization of the integer network is achieved for $\epsilon > 0.32$. By increasing the intralayer coupling strength, the interlayer synchrony is obtained for stronger ϵ. For example, for $\sigma = 0.2$ and 0.5, the network shows the interlayer synchronization for $\epsilon > 0.4$ and 0.48, respectively. When α changes to 0.9, no considerable change happens for the synchronization threshold for $\sigma = 0.05$ and 0.2. But the threshold for the stronger intralayer coupling strengths is influenced. It can be seen in Fig. 5b that the interlayer synchrony is obtained for $\epsilon > 0.4$ when $\sigma = 0.5$. Therefore, the dependence

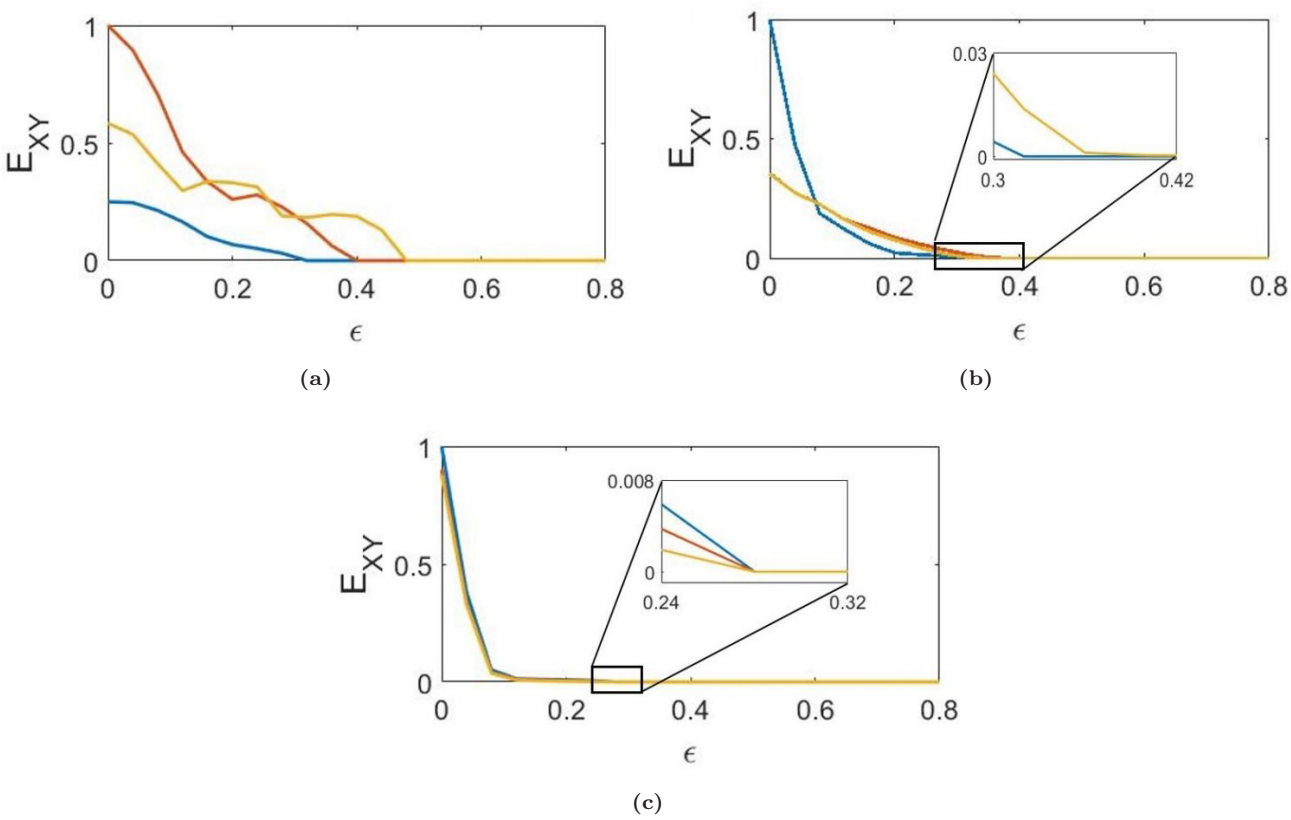

Fig. 5 The interlayer synchronization error according to interlayer coupling strength (ϵ), for different intralayer coupling strengths (blue: $\sigma = 0.05$, red: $\sigma = 0.2$, yellow: $\sigma = 0.5$). **(a)** $\alpha = 1$; **(b)** $\alpha = 0.9$; **(c)** $\alpha = 0.8$. The interlayer synchronization threshold is lessened by decreasing α.

of interlayer synchrony threshold on the intralayer coupling strength reduces for high σ values. With decrement of α to 0.8, the interlayer synchrony does not depend on the σ value and emerges for $\epsilon > 0.28$.

Next, we apply the master stability function for the synchronization between two layers. The synchronous manifold in this case is $S = X_i = Y_i$, which is obtained from the following equation:

$$D_t^\alpha S = F(S) + \sigma \sum_{j=1}^{N} G_{ij}^1 h(S). \tag{9}$$

Thus, the perturbation can be defined as $\eta_i = Y_i - X_i$. The derivative of the perturbation is $D_t^\alpha \eta_i = D_t^\alpha Y_i - D_t^\alpha X_i$, which leads to

$$D_t^\alpha \eta_i = F(Y_i) - F(X_i) - 2\epsilon H(\eta_i) + \sigma \sum_{j=1}^{N} G_{ij}^2 h(Y_j) - \sigma \sum_{j=1}^{N} G_{ij}^1 h(X_j). \tag{10}$$

Considering $\Delta G_{ij} = G_{ij}^2 - G_{ij}^1$, we have

$$D_t^\alpha \eta_i = F(Y_i) - F(X_i) - 2\epsilon H(\eta_i) + \sigma \sum_{j=1}^{N} G_{ij}^2 [h(Y_j) - h(X_j)] - \sigma \sum_{j=1}^{N} \Delta G_{ij} h(X_j), \tag{11}$$

which leads to the following linearized equation:

$$D_t^\alpha \eta_i = [JF(S_i) - 2\epsilon JH(S_i)]\eta_i + \sigma \sum_{j=1}^{N} G_{ij}^2 Jh(S_j)\eta_j - \sigma \sum_{j=1}^{N} \Delta G_{ij} h(S_j). \tag{12}$$

Since there is a slight difference between the topologies of the layers, we can neglect the term $\sigma \sum_{j=1}^{N} \Delta G_{ij} h(S_j)$ in the interlayer synchronization. Consequently, the sign of the MLE of Eq. (12), transverse to the synchronous manifold Eq. (9),

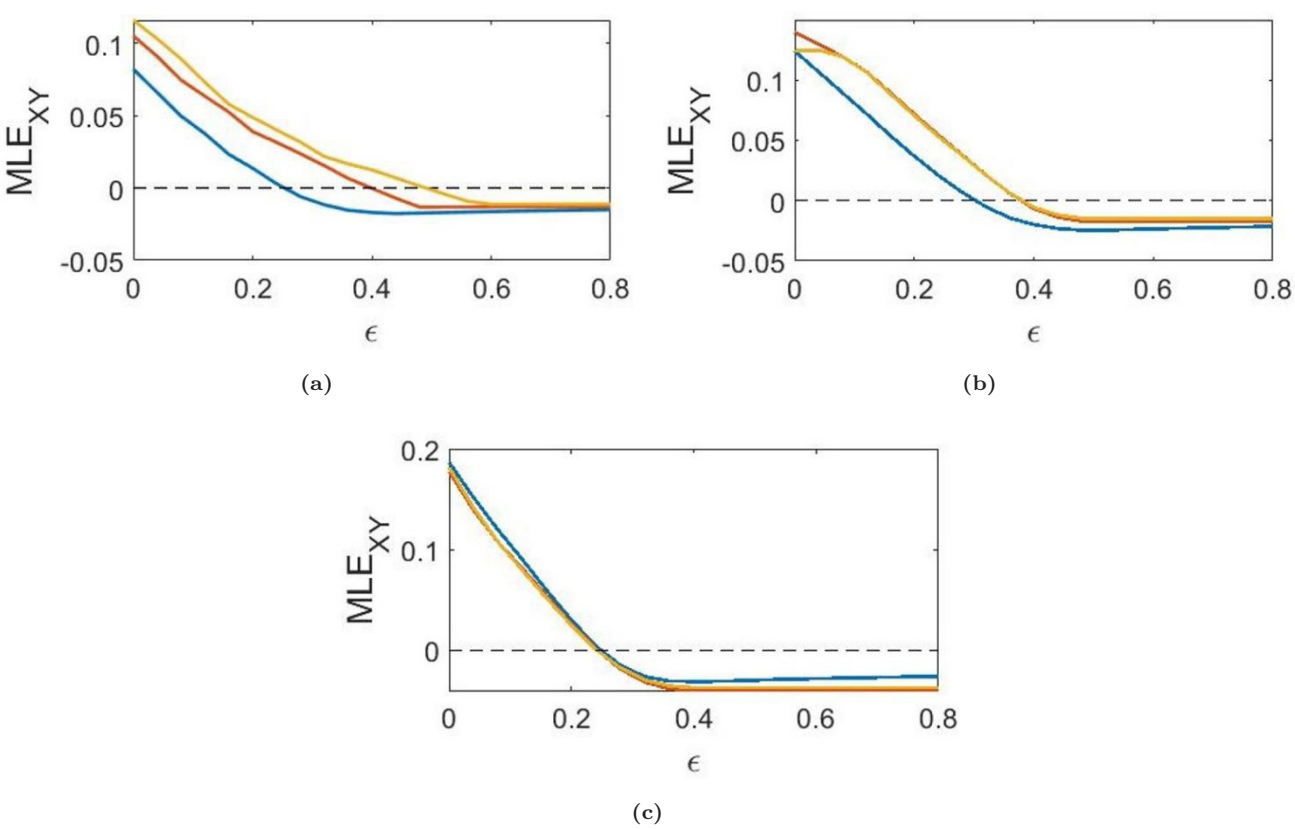

Fig. 6 The MLE of the linearized equations obtained for the interlayer synchronization (Eq. (12)) according to interlayer coupling strength (ϵ), for different intralayer coupling strengths (blue: $\sigma = 0.05$, red: $\sigma = 0.2$, yellow: $\sigma = 0.5$). **(a)** $\alpha = 1$; **(b)** $\alpha = 0.9$; **(c)** $\alpha = 0.8$.

determines the stability of the interlayer synchronization.

Figure 6 represents the MLE of Eq. (12) according to interlayer coupling strength. The figure demonstrates that the required ϵ for interlayer synchronization decreases with decreasing the derivative order. Furthermore, the dependence of the interlayer synchrony threshold on the intralayer coupling strength disappears.

4. CONCLUSION

This paper studied a multiplex network of HR models with fractional derivatives from the viewpoint of interlayer and intralayer synchronization. The small-world structure constructed each layer of the network, and both the interlayer and intralayer couplings were considered diffusive. The integer and fractional networks with different orders were solved numerically, and the averaged intralayer, and interlayer synchronization errors were calculated for different coupling strengths. Moreover, the master stability function was extended to obtain the necessary conditions for the interlayer and intralayer synchronizations in the multiplex fractional network. The results showed that for the integer network, the intralayer synchronization threshold first reduces and then increases with decreasing the interlayer coupling strength. In addition, the interlayer synchronization is achieved for stronger interlayer couplings as the intralayer coupling strength is enlarged. In comparison with the integer network, in the fractional network, both types of synchronizations were acquired in weaker couplings. By decreasing the order of the derivatives, the synchronization appeared within the layers in lower intralayer coupling strengths and between the layers in lower interlayer coupling strengths. Furthermore, the necessary interlayer (or intralayer) coupling strength for the interlayer (or intralayer) synchronization became independent of the intralayer (or interlayer) coupling strength.

ACKNOWLEDGMENTS

B. Yan was supported by the Natural Science Foundation of Hunan Province (No. 2021JJ40516). S. He was supported by the Natural Science Foundation of Hunan Province (No. 2020JJ5767) and the Natural Science Foundation of China (No. 61901530). M.P. was supported by the Slovenian Research Agency (Grant Nos. P1-0403 and J1-2457).

REFERENCES

1. A. Dzieliński, D. Sierociuk and G. Sarwas, Some applications of fractional order calculus, *Bull. Polish Acad. Sci. Tech. Sci.* **58** (2010) 583–592.
2. A. A. Khennaoui, A. Ouannas, S. Boulaaras, V.-T. Pham and A. T. Azar, A fractional map with hidden attractors: Chaos and control, *Eur. Phys. J. Spec. Top.* **229** (2020) 1083–1093.
3. A. Ouannas, A. A. Khennaoui, X. Wang, V.-T. Pham, S. Boulaaras and S. Momani, Bifurcation and chaos in the fractional form of Hénon–Lozi type map, *Eur. Phys. J. Spec. Top.* **229** (2020) 2261–2273.
4. S. He, S. Banerjee and K. Sun, Complex dynamics and multiple coexisting attractors in a fractional-order microscopic chemical system, *Eur. Phys. J. Spec. Top.* **228** (2019) 195–207.
5. S. Boulaaras, F. Kamache, Y. Bouizem and R. Guefaifia, General decay and blow-up of solutions for a nonlinear wave equation with memory and fractional boundary damping terms, *Boundary Value Probl.* **2020** (2020) 172.
6. D. Kumar and D. Baleanu, Fractional calculus and its applications in physics, *Front. Phys.* **7** (2019) 81.
7. J. Sabatier, P. Lanusse, P. Melchior and A. Oustaloup, Fractional order differentiation and robust control design, *Intelligent Systems, Control and Automation: Science and Engineering*, Vol. 77 (Springer, 2015), pp. 13–18.
8. K. Rajagopal, N. Hasanzadeh, F. Parastesh, I. I. Hamarash, S. Jafari and I. Hussain, A fractional-order model for the novel coronavirus (COVID-19) outbreak, *Nonlinear Dynam.* **101** (2020) 711–718.
9. Z. Wang, X. Wang, Y. Li and X. Huang, Stability and Hopf bifurcation of fractional-order complex-valued single neuron model with time delay, *Int. J. Bifurcation Chaos* **27** (2017) 1750209.
10. S. He, K. Sun and H. Wang, Complexity analysis and DSP implementation of the fractional-order Lorenz hyperchaotic system, *Entropy* **17** (2015) 8299–8311.
11. S. H. Weinberg, Membrane capacitive memory alters spiking in neurons described by the fractional-order Hodgkin–Huxley model, *PLoS One* **10** (2015) e0126629.
12. W. W. Teka, R. K. Upadhyay and A. Mondal, Spiking and bursting patterns of fractional-order Izhikevich model, *Commun. Nonlinear Sci. Numer. Simul.* **56** (2018) 161–176.
13. E. Kaslik, Analysis of two-and three-dimensional fractional-order Hindmarsh–Rose type neuronal models, *Fract. Calc. Appl. Anal.* **20** (2017) 623–645.

14. J. Guo, Y. Yin, X. Hu and G. Ren, Self-similar network model for fractional-order neuronal spiking: Implications of dendritic spine functions, *Nonlinear Dynam.* **100** (2020) 921–935.
15. A. Mondal, S. K. Sharma, R. K. Upadhyay and A. Mondal, Firing activities of a fractional-order FitzHugh–Rinzel bursting neuron model and its coupled dynamics, *Sci. Rep.* **9** (2019) 15721.
16. D. Jun, Z. Guang-jun, X. Yong, Y. Hong and W. Jue, Dynamic behavior analysis of fractional-order Hindmarsh–Rose neuronal model, *Cogn. Neurodyn.* **8** (2014) 167–175.
17. S. Boccaletti, J. Kurths, G. Osipov, D. Valladares and C. Zhou, The synchronization of chaotic systems, *Phys. Rep.* **336** (2002) 1–101.
18. S. L. Bressler and C. G. Richter, Interareal oscillatory synchronization in top-down neocortical processing, *Curr. Opin. Neurobiol.* **31** (2015) 62–66.
19. S. Rakshit, A. Ray, B. K. Bera and D. Ghosh, Synchronization and firing patterns of coupled Rulkov neuronal map, *Nonlinear Dynam.* **94** (2018) 785–805.
20. F. Parastesh, H. Azarnoush, S. Jafari, B. Hatef, M. Perc and R. Repnik, Synchronizability of two neurons with switching in the coupling, *Appl. Math. Comput.* **350** (2019) 217–223.
21. F. Wu, J. Ma and G. Zhang, Energy estimation and coupling synchronization between biophysical neurons, *Sci. China Technol. Sci.* **63** (2020) 625–636.
22. I. Belykh, E. de Lange and M. Hasler, Synchronization of bursting neurons: What matters in the network topology, *Phys. Rev. Lett.* **94** (2005) 188101.
23. M. Uzuntarla, J. J. Torres, A. Calim and E. Barreto, Synchronization-induced spike termination in networks of bistable neurons, *Neural Netw.* **110** (2019) 131–140.
24. J. Ma, L. Mi, P. Zhou, Y. Xu and T. Hayat, Phase synchronization between two neurons induced by coupling of electromagnetic field, *Appl. Math. Comput.* **307** (2017) 321–328.
25. Y. Zhao, X. Sun, Y. Liu and J. Kurths, Phase synchronization dynamics of coupled neurons with coupling phase in the electromagnetic field, *Nonlinear Dynam.* **93** (2018) 1315–1324.
26. M. Shafiei, F. Parastesh, M. Jalili, S. Jafari, M. Perc and M. Slavinec, Effects of partial time delays on synchronization patterns in Izhikevich neuronal networks, *Eur. Phys. J. B* **92** (2019) 36.
27. I. Hussain, D. Ghosh and S. Jafari, Chimera states in a thermosensitive FitzHugh–Nagumo neuronal network, *Appl. Math. Comput.* **410** (2021) 126461.
28. E. Yilmaz, M. Ozer, V. Baysal and M. Perc, Autapse-induced multiple coherence resonance in single neurons and neuronal networks, *Sci. Rep.* **6** (2016) 30914.
29. V. Vafaei, H. Kheiri and A. J. Akbarfam, Synchronization of fractional-order chaotic systems with disturbances via novel fractional-integer integral sliding mode control and application to neuron models, *Math. Methods Appl. Sci.* **42** (2019) 2761–2773.
30. D. Liu, S. Zhao, X. Luo and Y. Yuan, Synchronization for fractional-order extended Hindmarsh–Rose neuronal models with magneto-acoustical stimulation input, *Chaos Solitons Fractals* **144** (2021) 110635.
31. L. Chen, J. Cao, R. Wu, J. T. Machado, A. M. Lopes and H. Yang, Stability and synchronization of fractional-order memristive neural networks with multiple delays, *Neural Netw.* **94** (2017) 76–85.
32. Y. Xie, Y. Kang, Y. Liu and Y. Wu, Firing properties and synchronization rate in fractional-order Hindmarsh–Rose model neurons, *Sci. China Technol. Sci.* **57** (2014) 914–922.
33. S. Malik and A. Mir, Synchronization of fractional order neurons in presence of noise, in *IEEE/ACM Transactions on Computational Biology and Bioinformatics* (IEEE, 2022), pp. 1887–1896.
34. T. A. Giresse, K. T. Crepin and T. Martin, Generalized synchronization of the extended Hindmarsh–Rose neuronal model with fractional order derivative, *Chaos Solitons Fractals* **118** (2019) 311–319.
35. F. Meng, X. Zeng and Z. Wang, Dynamical behavior and synchronization in time-delay fractional-order coupled neurons under electromagnetic radiation, *Nonlinear Dynam.* **95** (2019) 1615–1625.
36. S. Boccaletti, V. Latora, Y. Moreno, M. Chavez and D.-U. Hwang, Complex networks: Structure and dynamics, *Phys. Rep.* **424** (2006) 175–308.
37. S. Boccaletti, G. Bianconi, R. Criado, C. I. Del Genio, J. Gómez-Gardenes, M. Romance, I. Sendina-Nadal, Z. Wang and M. Zanin, The structure and dynamics of multilayer networks, *Phys. Rep.* **544** (2014) 1–122.
38. I. Belykh, D. Carter and R. Jeter, Synchronization in multilayer networks: When good links go bad, *SIAM J. Appl. Dyn. Syst.* **18** (2019) 2267–2302.
39. F. Della Rossa, L. Pecora, K. Blaha, A. Shirin, I. Klickstein and F. Sorrentino, Symmetries and cluster synchronization in multilayer networks, *Nat. Commun.* **11** (2020) 3179.
40. F. Drauschke, J. Sawicki, R. Berner, I. Omelchenko and E. Schöll, Effect of topology upon relay synchronization in triplex neuronal networks, *Chaos* **30** (2020) 051104.
41. F. Xu, J. Zhang, M. Jin, S. Huang and T. Fang, Chimera states and synchronization behavior in multilayer memristive neural networks, *Nonlinear Dynam.* **94** (2018) 775–783.
42. M. Shafiei, S. Jafari, F. Parastesh, M. Ozer, T. Kapitaniak and M. Perc, Time delayed chemical synapses

and synchronization in multilayer neuronal networks with ephaptic inter-layer coupling, *Commun. Nonlinear Sci. Numer. Simul.* **84** (2020) 105175.

43. S. Rakshit, B. K. Bera and D. Ghosh, Synchronization in a temporal multiplex neuronal hypernetwork, *Phys. Rev. E* **98** (2018) 032305.
44. K. Diethelm and A. D. Freed, The FracPECE subroutine for the numerical solution of differential equations of fractional order, *Forsch. Wiss. Rechnen* **1999** (1998) 57–71.